Numerical Simulation to Analyze Statistical Variation of Creep of Concrete

Tatsuya TSUBAKI, Monoj Kanti DAS, Kazushige SHITABA
Yokohama National University, Yokohama, Japan

ABSTRACT

The statisitical variation involved in creep of concrete is investigated by using a numerical simulation method with concrete elements. It becomes clear that the use of concrete elements is effective to simulate the time-dependent mechanical behavior of concrete.

1 INTRODUCTION

It has been pointed out that the time-dependent material property of concrete such as creep and shrinkage involve a large statistical variation. There are two kinds of factors which cause such a statistical variation, i.e., internal factors such as the variation in the mix-proportions of concrete and external factors such as the environmental humidity and temperature(cf. Tsubaki, et al. (1988)). Considering the 'apparent' internal mechanisms of creep for the mesostructure of concrete(cf. Young, et al.(1988)), the effect of the spatial distribution of coarse aggregates is investigated in this study under various conditions by a numerical simulation for two-dimensional numerical concrete specimens.

2 METHOD OF ANALYSIS USING CONCRETE ELEMENT

Although there are several methods(cf. Roelfstra, et al.(1985)), the concept of a concrete element(cf. Tsubaki, et al.(1990)) is used in this study because of efficiency in computation. Assuming that concrete is modeled as a composite material which is made up of mortar and aggregates(cf. Fig. 1), a concrete element is composed of three parts, i.e., mortar, an coarse aggregate and the interface region between them(cf. Fig. 2). The incremental stiffness equation for the finite element method is given as follows in general.

$$\mathbb{K}\,d\mathbb{U} = d\mathbb{F} + d\mathbb{F}'' \tag{1}$$

where $\mathbb{K}$, $\mathbb{U}$, $\mathbb{F}$ and $\mathbb{F}''$ stand for the element stiffness matrix, the displacement vector, the load vector, and the equivalent load vector due to inelastic strains, etc., respectively. $\mathbb{F}''$ can take into account the effect of the viscoelastic-plastic behavior and cracking of mortar, the elastic behavior with cracking of aggregate, and the frictional slip and the separation of the interface region in case of interfacial cracking. Eq.(1) is decomposed into two parts which are related to the external and internal nodes of a concrete element as follows.

$$\begin{bmatrix} \mathbb{K}_{EE} & \mathbb{K}_{EI} \\ \mathbb{K}_{IE} & \mathbb{K}_{II} \end{bmatrix} \begin{Bmatrix} d\mathbb{U}_E \\ d\mathbb{U}_I \end{Bmatrix} = \begin{Bmatrix} d\mathbb{F}_E \\ d\mathbb{F}_I \end{Bmatrix} + \begin{Bmatrix} d\mathbb{F}''_E \\ d\mathbb{F}''_I \end{Bmatrix} \tag{2}$$

where subscripts E and I stand for the quantities related to external and internal nodes, respectively. Assuming that external loads are not applied to the internal nodes, $\mathbb{F}_I = \mathbb{0}$ holds. Then, the stiffness equation for the external nodes only is derived as follows.

$$\bar{\mathbb{K}} d\mathbb{U}_E = d\bar{\mathbb{F}} \; ; \; \bar{\mathbb{K}} = \mathbb{K}_{EE} - \mathbb{K}_{EI}\mathbb{K}_{II}^{-1}\mathbb{K}_{IE} \tag{3a, b}$$

$$d\bar{\mathbb{F}} = d\mathbb{F}_E + d\mathbb{F}''_E - \mathbb{K}_{EI}\mathbb{K}_{II}^{-1}d\mathbb{F}''_I \; ; \; d\mathbb{U}_I = \mathbb{K}_{II}^{-1}(d\mathbb{F}''_I - \mathbb{K}_{IE}d\mathbb{U}_E) \tag{4a, b}$$

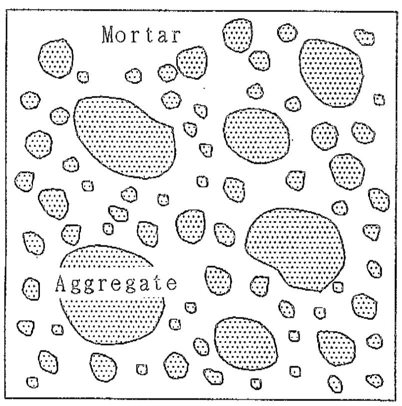

Fig. 1 Internal structure of concrete

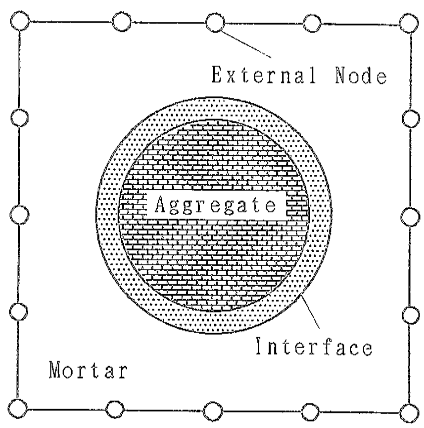

Fig. 2 Concrete element

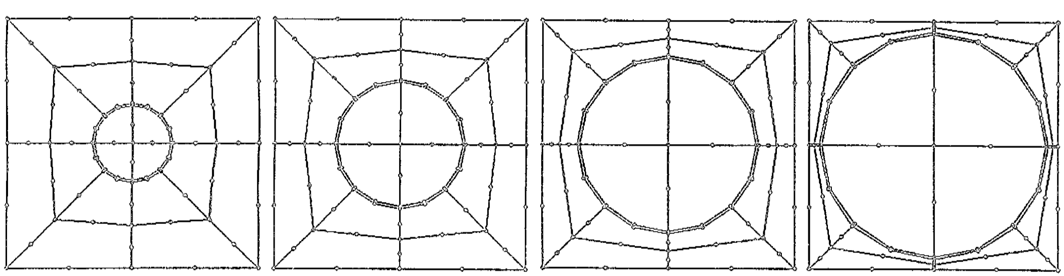

(a) D/L=0.3 (b) D/L=0.5 (c) D/L=0.7 (d) D/L=0.9

Fig. 3 Various types of concrete element

Eq.(4b) is used to obtain the internal nodal displacements. The concrete elements used in this study are shown in Fig. 3 where D and L stand for the diameter of the aggregate and the side length, respectively. Each concrete element has 16 external nodes, 77 internal nodes and 28 internal elements. 8-node isoparametric elements are used for internal elements.

3 NUMERICAL EXAMPLES

The concrete specimen considered in this study is a rectangle(20 cm x 10 cm). The size of a concrete element is 2 cm. The element discretization is shown in Fig. 4(a). The total number of nodes is 4261 and the total number of elements is 1400. In order to take into account the effect of environmental conditions, the moisture diffusion in concrete is analyzed. The humidity dependency of the diffusion coefficient is modeled by the equation proposed by Bažant, et al.(1972), with C_1=0.3 cm^2/day, H_c=0.75, α_0=0.05, n=16. The initial pore humidity is H_0=100 % and the environmental humidity is H_{en}=70 %. Fig. 4(b) shows the humidity distribution for drying time $t-t_0$=10 days. Inhomogeneous humidity distribution is observed because of the effect of spatial distribution of aggregates. The creep behavior of numerical concrete specimens is analyzed for three cases: (a) basic creep(case-1) with $E_M=E_I=2\times10^3$ Kgf/cm^2, $\nu_M=\nu_I=0.4$, $\phi_M=\phi_I=1$; (b) basic creep(case-2) with $E_M=E_I=2\times10^5$ Kgf/cm^2, $\nu_M=\nu_I=0.2$, $\phi_M=\phi_I=3$; (c) drying creep with the same material properties as case (b) and drying condition shown in Fig. 4(b). In all cases, $E_A=10E_M$, $\nu_A=0.2$, $\phi_A=0$, subscripts M, I, A stand for mortar, interface and aggregate, and ϕ is the creep coefficient to indicate the total amount of creep strain. Case (a) simulates early age concrete, while case(b) is for hardened concrete. The load is applied to the upper surface, keeping the vertical displacements of the loading surface constant. The lateral constraints along the loading surface and the lower surface are assumed negligible. Also, in case (c), it is assumed that the unrestrained incremental shrinkage of mortar is linearly proportional to the incremental change of humidity and the proportional constant is $\kappa=1.6\times10^{-3}$ (cf. Neville

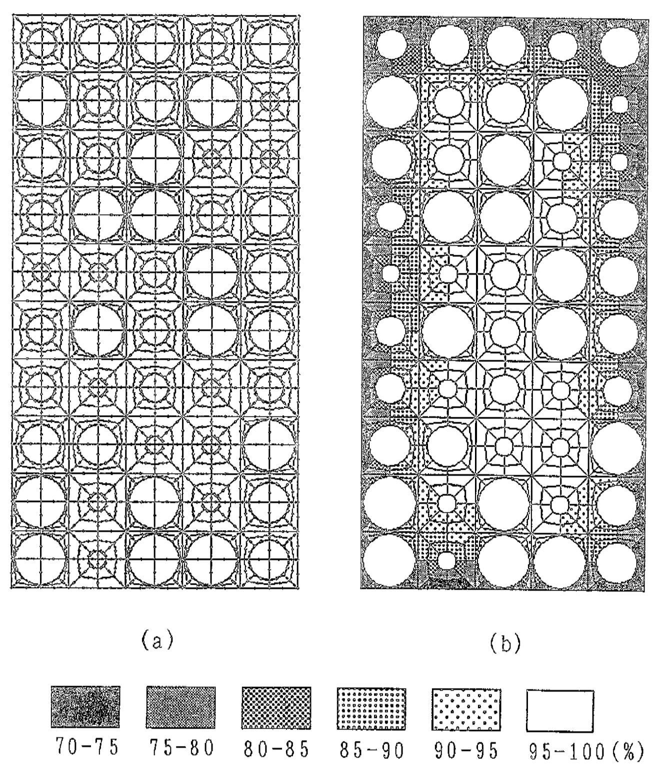

Fig. 4 Modeling of concrete specimen: (a) Element discretization; (b) Drying condition

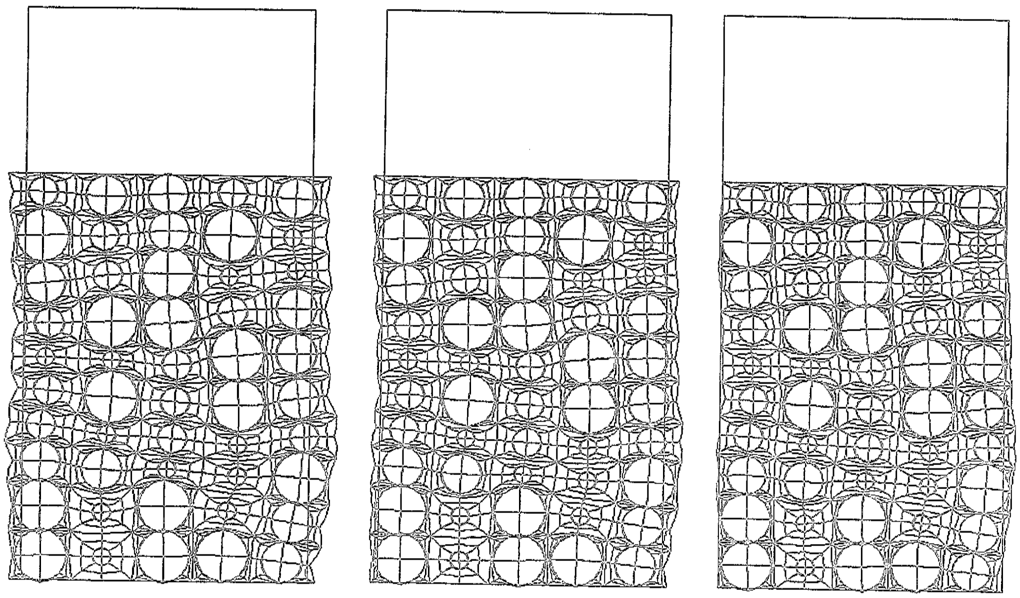

(a) Basic creep(Case-1)　(b) Basic creep(Case-2)　(c) Drying creep

Fig. 5 Creep deformation of concrete

(1981) and Wittmann(1985)). The displacement diagrams of numerical concrete specimens for these conditions are shown in Fig. 5. Large lateral creep deformation is observed in case (a). In case (c), lateral deformation is reduced due to shrinkage. Changing the spatial distribution of aggregates randomly, 30 numerical specimens are analyzed for cases (a) and (b), and 10 numerical specimens for case (c). The longitudinal specific creep strain is calculated from the vertical displacements at two nodes which are on the lateral surfaces and one-fourth of the height of the specimen apart from the upper and lower surfaces. The variation of the longitudinal creep strain is shown in Fig. 6. The mean value and the coefficient of variation are summarized in Table 1. A considerable amount of statisitcal variation is observed for all cases. The distributions of the lateral creep strain and the normal stresses acting on the upper and lower surfaces are shown in Fig. 7. All quantities in Fig. 7 are normalized by their mean values shown in Table 1. The normalized position indicates the

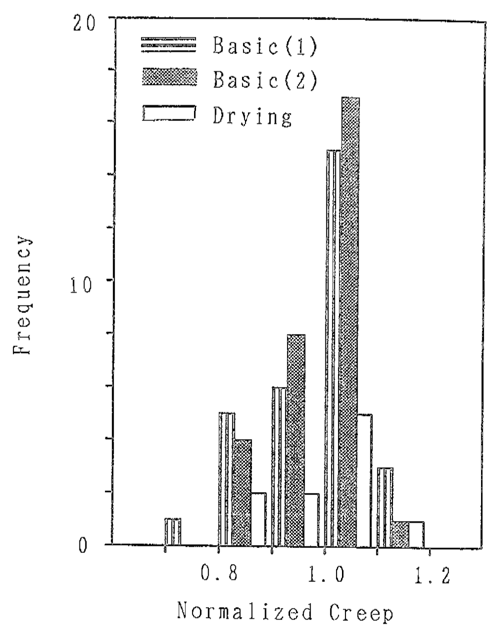

Fig. 6 Variation of longitudinal creep strain

relative distance from the end point of the surface. From Fig. 7(a), it is confirmed that the mean value of the lateral creep is restrained and its statistical variation becomes large because of the existence of aggregates. Due to drying, both the mean value and the coefficient of variation of the lateral creep strain become significantly large. The normal stresses acting on the upper and lower surfaces are almost constant for all cases, while the distributions of the coefficients of variation are not uniform.

4 CONCLUSIONS

By a numerical simulation for the creep deformation of concrete, it becomes

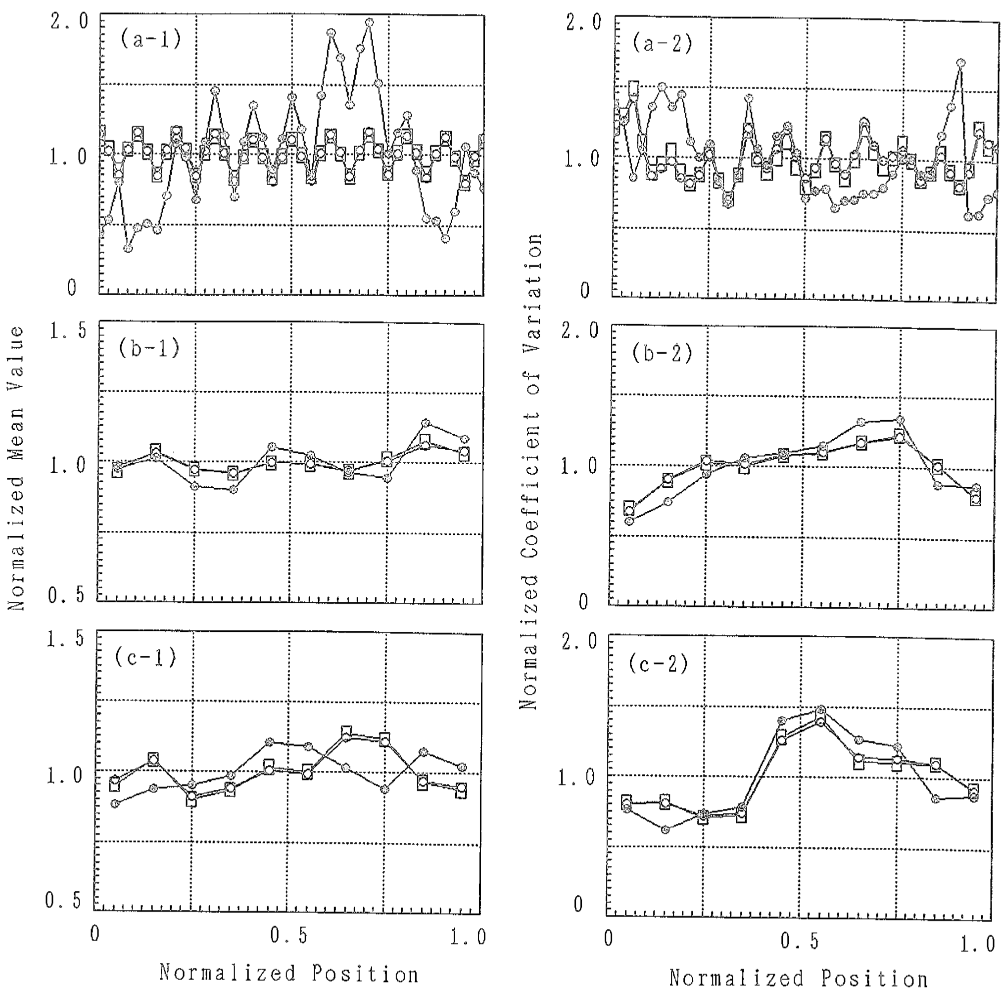

Fig. 7 Distribution of Mean value and coefficient of variation of creep and stress for various conditions: (a) Lateral creep; (b) Stress(Upper side); (c) Stress(Lower side) [□=Basic creep(Case-1), ○=Basic creep (Case-2), ●=Drying creep]

Table 1. Mean value and coefficient of variation of creep and stress for various conditions

Drying Condition	Basic Creep (Case-1)	Basic Creep (Case-2)	Drying Creep
Longitudinal Creep [1/(Kgf/cm^2)]	4.884×10^{-4} (16.47%)	1.050×10^{-5} (14.82%)	1.157×10^{-5} (15.83%)
Lateral Creep [1/(Kgf/cm^2)]	1.639×10^{-4} (23.32%)	2.025×10^{-6} (22.09%)	6.161×10^{-7} (63.13%)
Stress(Upper Side) [Kgf/cm^2]	2.053 (32.68%)	95.46 (29.23%)	83.21 (28.65%)
Stress(Lower Side) [Kgf/cm^2]	2.053 (34.08%)	95.46 (29.97%)	83.21 (34.20%)

[Note] Numbers in parentheses are coefficients of variation.

clear that a part of the statistical variation of creep may be attributed to the random spatial distribution of coarse aggregates. Also, it is confirmed that the simulation method based on the concept of a concrete element is efficient for this kind of numerical simulation. The use of concrete elements reduces the number of degrees of freedom needed in the analysis and is convenient for the element discretization of a composite material such as concrete.

REFERENCES

Bažant, Z.P. and Najjar, L.J. (1972). Nonlinear Water Diffusion in Nonsaturated Concrete, Materials and Structures, Vol.5, pp.3-20.

Neville, A.M. (1981). Properties of Concrete, 3rd Ed., London, Pitman.

Roelfstra, P.E., Sadouki, H. and Wittmann, F.H. (1985). Le beton numerique, Materials and Structures, Vol.18, pp.327-336.

Tsubaki, T., et al. (1988). Probabilistic Models, Chap.5, Mathematical Modeling of Creep and Shrinakge of Concrete, Ed. by Z.P. Bažant, Wiley, pp.311-383.

Tsubaki, T. and Shitaba, K. (1990). On the FEM Simulation of the Material Properties of Concrete, Proc. of Symp. on Computational Methods in Structural Engineering and Related Fields, Vol.14, pp.425-430. (in Japanese)

Wittmann, F.H. (1985). Deformation of Concrete at Variable Moisture Content, Chap.19, Mechanics of Geomaterials, Ed. by Z.P. Bažant, Wiley, pp.425-459.

Young, J.F., et al. (1988). Physical Mechanisms and Their Mathematical Description, Chap.1, Mathematical Modeling of Creep and Shrinkage of Concrete, Ed. by Z.P. Bažant, Wiley, pp.63-98.